Journal of Sound and Vibration (2002) **254**(5), 967–986
doi:10.1006/jsvi.2001.4140, available online at http://www.idealibrary.com on IDEAL®

IDENTIFICATION OF SPEED-DEPENDENT BEARING PARAMETERS

R. Tiwari†, A. W. Lees and M. I. Friswell

Department of Mechanical Engineering, University of Wales Swansea, Swansea SA2 8PP, U.K. E-mails: r.tiwari@swansea.ac.uk, a.w.lees@swansea.ac.uk, m.i.friswell@swansea.ac.uk

(*Received* 30 *July* 2001, *and in final form* 22 *October* 2001)

Bearing dynamic characteristics have been a major unknown in the modelling and analysis of large turbo-generators. An identification algorithm for bearing dynamic characterization by using unbalance response measurements is developed for multi-degree-of-freedom (m.d.o.f.) flexible rotor-bearing systems. The algorithm identifies the bearing dynamic parameters, consisting of four effective stiffness and four damping coefficients for each bearing, utilizing frequency domain synchronous unbalance response measurements from the accelerometers attached to the bearing housings in the horizontal and vertical directions, for a minimum two different unbalance configurations. The procedure of identifying bearing dynamic coefficients by using the proposed algorithm is presented and demonstrated through a numerical example. Adding noise to the simulated signal checks the robustness of the algorithm against measurement noise. Combinations of regularization and the generalized singular value decomposition (SVD) are used to tackle an ill-posed problem due to the nearly circular orbit of the rotor at the bearings, as a special case for nearly isotropic bearings. It is demonstrated that by measuring noisy bearing responses with the direction of rotation of the rotor both in the clockwise and anticlockwise directions, the bearing estimation problem for circular orbit becomes well-conditioned. The regularization algorithm is tested for an experimental rotor-bearing rig. The response reproduction capabilities are excellent even in the presence of measurement noise.

1. INTRODUCTION

In modern power plants, because of ever-increasing demand for high power and high speed with uninterrupted and reliable operation, the accurate prediction of the dynamic behaviour of such machinery has become increasingly important. The most crucial part of such large turbo-generators is the machine elements that allow relative motion between the rotating and the stationary machine elements, i.e., the bearings. Historically, the theoretical estimates of the dynamic bearing characteristics have always been a source of error in the prediction of dynamic behaviour of rotor-bearing systems. Consequently, accurate parameter identification is required to reduce the discrepancy between the measurements and the predictions. In particular, physically meaningful experimental identification of bearing dynamic coefficients is necessary because of the difficulty in accurate system modelling and analysis [1].

Obtaining reliable estimates of the bearing static load in actual test conditions is quite difficult and this leads to inaccuracies in the well-established theoretical bearing models.

† Parent Institution: Department of Mechanical Engineering, Indian Institute of Technology, Guwahati 781039, India (rtiwari@iitg.ernet.in).

0022-460X/02/$35.00

Hence, the estimation of bearing dynamic parameters in actual test conditions is important to rotor design. Mitchell *et al.* [2] obtained the stiffness of an oil film bearing experimentally, by application of *static loads*. Morton [3] devised the measurement procedure for estimation of the dynamic characteristics of a large sleeve bearing by application of *dynamic loads* (sinusoidal excitation at a frequency non-synchronous with the running frequency of the sleeve) using vibrators, whilst Childs and Hale [4] devised a test apparatus and facility to identify the rotordynamic coefficients of high-speed hydrostatic bearings (with shakers to provide sinusoidal excitation along two perpendicular directions). Nordmann and Schollhorn [5] identified the stiffness and damping coefficients of journal bearings whereas Kraus *et al.* [6] identified the coefficients for rolling element bearings by means of *the impact method*. Sahinkaya and Burrows [7] and Tieu and Qiu [8] estimated the linearized oil film parameters from the out-of-balance response where the shaft was excited by a *known unbalance force* (synchronous excitation). Chen and Lee [9] identified rolling element dynamic characteristics in flexible rotor-bearing systems by using unbalance responses at all bearings and several shaft locations without *a priori* knowledge of the unbalance. Muszynska and Bently [10] developed a *perturbation technique* (two frequency swept periodic inputs) for estimation of these parameters. Tiwari and Vyas [11] extracted the non-linear stiffness parameters of rolling element bearings based on the *natural random response* at the bearings of rotor-bearing systems. Goodwin [12] reviewed the experimental approaches to rotor support impedance measurement. Swanson and Kirk [13] presented a survey in tabular form of the experimental data available in the open literature for fixed geometry hydrodynamic journal bearings.

Most of the bearing parameter identification methods available require the bearing to be tested in isolation or in a rotor-bearing system where the shaft is rigid. Very few researchers have considered the flexibility of the shaft. The present method develops a bearing parameter identification algorithm for m.d.o.f. rotor-bearing systems treating the shaft as flexible and has bearings with speed-dependent parameters. From the dynamic stiffness equation of a rotor-bearing system a general algorithm is derived to extract bearing parameters. From a minimum of two run-downs with different unbalance configurations, speed-dependent bearing dynamic parameters are identified. A numerical simulation illustrates the algorithm and checks the robustness against measurement noise. For nearly isotropic bearings when the shaft orbit becomes nearly circular at the bearings, combinations of regularization and the generalized SVD techniques are used to solve an ill-posed problem. For circular orbits, it is demonstrated that by measuring noisy bearing responses with the direction of rotation of the rotor both in the clockwise and anticlockwise directions, the bearing estimation problem becomes well-conditioned. The present regularization algorithm is tested using an experimental rotor-bearing rig.

2. THEORY

Figure 1 shows a flexible rotor supported on flexible bearings with rigid foundations. The dynamic stiffness equation in the frequency domain for the m.d.o.f. rotor-bearing system is

$$\begin{bmatrix} \mathbf{D}_{R,ii} & \mathbf{D}_{R,ib} \\ \mathbf{D}_{R,bi} & (\mathbf{D}_{R,bb} + \mathbf{D}_{B,bb}) \end{bmatrix} \begin{Bmatrix} \mathbf{z}_{R,i} \\ \mathbf{z}_{R,b} \end{Bmatrix} = \begin{Bmatrix} \mathbf{f}_u \\ 0 \end{Bmatrix}, \tag{1}$$

where $\mathbf{D}$ is the dynamic stiffness, $\mathbf{f}_u$ is the unbalance force, the first subscript, R or B, refers to the rotor and bearing, respectively, and the second subscript, i or b, corresponds to the internal and connection degrees of freedom (d.o.f.s) respectively. The d.o.f.s of the rotor at the bearing locations are called connection d.o.f.s, $\mathbf{z}_{R,b}$, and the d.o.f.s of the rotor other

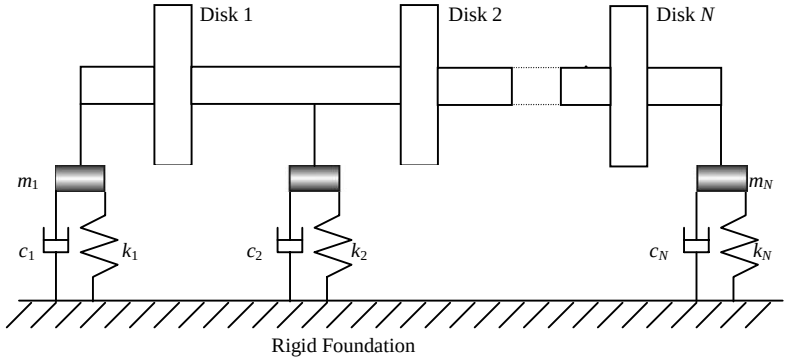

Figure 1. Schematic diagram of the flexible rotor-bearings system.

than at the bearing locations are called internal d.o.f.s, $\mathbf{z}_{R,i}$. Appendix B gives a list of nomenclature. It is assumed here that balance planes (unbalances) are present only at the rotor internal d.o.f. Equation (1) may be expanded as

$$\mathbf{D}_{R,ii}\,\mathbf{z}_{R,i} + \mathbf{D}_{R,ib}\,\mathbf{z}_{R,b} = \mathbf{f}_u \tag{2}$$

and

$$\mathbf{D}_{R,bi}\,\mathbf{z}_{R,i} + (\mathbf{D}_{R,bb} + \mathbf{D}_{B,bb})\mathbf{z}_{R,b} = 0. \tag{3}$$

Equation (2) may be rearranged to give the rotor internal d.o.f. response as

$$\mathbf{z}_{R,i} = \mathbf{D}_{R,ii}^{-1}[\mathbf{f}_u - \mathbf{D}_{R,ib}\,\mathbf{z}_{R,b}]. \tag{4}$$

Equation (4) may be used to give the rotor internal d.o.f. response for known unbalance, rotor model and bearing connection d.o.f. response. Equation (3) may be rearranged as

$$\mathbf{D}_{B,bb}\,\mathbf{z}_{R,b} = -\mathbf{D}_{R,bi}\,\mathbf{z}_{R,i} - \mathbf{D}_{R,bb}\,\mathbf{z}_{R,b}. \tag{5}$$

Equation (5) may be represented as

$$[\mathbf{K}_B(\omega) + (\mathrm{j}\omega)^2\mathbf{M}_B(\omega) + \mathrm{j}\omega\mathbf{C}_B(\omega)]\,\mathbf{z}_{R,b}(\omega) = \mathbf{P}(\omega), \tag{6}$$

where

$$\mathbf{P}(\omega) = -\mathbf{D}_{R,bi}\,\mathbf{z}_{R,i} - \mathbf{D}_{R,bb}\,\mathbf{z}_{R,b}\,. \tag{7}$$

In equation (6), $\mathbf{K}_B$, $\mathbf{C}_B$ and $\mathbf{M}_B$ represent bearing stiffness, damping and mass matrices, respectively, ω represents the rotor speed and $\mathrm{j} = \sqrt{-1}$. Separating the real and imaginary parts of equation (6) yields

$$[\mathbf{K}_B(\omega) - \omega^2\mathbf{M}_B(\omega)]\,\mathbf{z}^r_{R,b}(\omega) - \omega\mathbf{C}_B(\omega)\mathbf{z}^i_{R,b}(\omega) = \mathbf{P}^r(\omega) \tag{8}$$

and

$$[\mathbf{K}_B(\omega) - \omega^2\mathbf{M}_B(\omega)]\,\mathbf{z}^i_{R,b}(\omega) + \omega\mathbf{C}_B(\omega)\mathbf{z}^r_{R,b}(\omega) = \mathbf{P}^i(\omega). \tag{9}$$

where superscripts r and i represent the real and imaginary parts respectively. Note that the K_B, C_B and M_B matrices are block diagonal, which means that the identification may be performed on a *per bearing* basis. Equations (8) and (9) may be combined, for each bearing, to give

$$[\mathbf{B}^j_0(\omega)\mathbf{B}^j_1(\omega)]\,\beta^j(\omega) = \mathbf{q}^j(\omega), \tag{10}$$

where

$$\mathbf{B}_0^j(\omega) = \begin{bmatrix} x_j^r(\omega) & y_j^r(\omega) & 0 & 0 \\ 0 & 0 & x_j^r(\omega) & y_j^r(\omega) \\ x_j^i(\omega) & y_j^i(\omega) & 0 & 0 \\ 0 & 0 & x_j^i(\omega) & y_j^i(\omega) \end{bmatrix}, \tag{11}$$

$$\mathbf{B}_1^j(\omega) = \omega \begin{bmatrix} -x_j^i(\omega) & -y_j^i(\omega) & 0 & 0 \\ 0 & 0 & -x_j^i(\omega) & -y_j^i(\omega) \\ x_j^r(\omega) & y_j^r(\omega) & 0 & 0 \\ 0 & 0 & x_j^r(\omega) & y_j^r(\omega) \end{bmatrix}, \tag{12}$$

$$\mathbf{q}^j(\omega) = \{P^r_{2j-1}(\omega)\ P^r_{2j}(\omega)\ P^i_{2j-1}(\omega)\ P^i_{2j}(\omega)\}^{\mathrm{T}}, \tag{13}$$

$$\boldsymbol{\beta}^j(\omega) = \{k^j_{xx}(\omega) \quad k^j_{xy}(\omega) \quad k^j_{yx}(\omega) \quad k^j_{yy}(\omega) \quad c^j_{xx}(\omega) \quad c^j_{xy}(\omega) \quad c^j_{yx}(\omega) \quad c^j_{yy}(\omega)\}^{\mathrm{T}} \tag{14}$$

and

$$j = 1, 2, \ldots, n_b. \tag{15}$$

k and c represent the bearing effective stiffness and damping coefficients, respectively, x_j and y_j represent the jth bearing responses in the horizontal and vertical directions, respectively, and n_b represents total number of bearings in the rotor-bearing system. In equation (14) stiffness and mass terms are combined during estimation. The estimation of stiffness and mass terms separately would lead the regression matrix, $\mathbf{B}$ (see equation (17)) to be singular. The combined stiffness and mass term, $(k - \omega^2 m)$, is referred to as the *speed-dependent effective stiffness*, k. Equation (10) may be written for the jth bearing at a particular speed ω_i and for the nth unbalance configuration run-down as

$$^n\mathbf{B}^j(\omega_i)\boldsymbol{\beta}^j(\omega_i) = {}^n\mathbf{q}^j(\omega_i) \tag{16}$$

which can be combined for different unbalance configuration run-downs (say m) at the same speed to yield

$$\mathbf{B}^j(\omega_i)\boldsymbol{\beta}^j(\omega_i) = \mathbf{q}^j(\omega_i), \tag{17}$$

where

$$\begin{aligned} \mathbf{B}^j &= [{}^1B^j \quad {}^2B^j \ \cdots \ {}^mB^j]^{\mathrm{T}}, \\ \mathbf{q}^j &= [{}^1q^j \quad {}^2q^j \ \cdots \ {}^mq^j]^{\mathrm{T}}, \end{aligned} \quad m \geqslant 2; j = 1, 2, \ldots, n_b. \tag{18}$$

Equation (17) may be used to obtain speed-dependent bearing parameters using the ordinary least-squares estimation technique in conjunction with the regularization techniques described below. A minimum of two run-down responses with different unbalance configurations (both at the bearing locations and the rotor internal d.o.f. locations) are required for the identification of bearing parameters for any number of bearings. If the rotor internal d.o.f. can be measured then the estimates of rotor unbalance will not be required in the estimation algorithm. This may be suitable for a laboratory type rotor-bearing set-up but requires significant measurement sensors and related signal conditioning hardware. If the rotor internal d.o.f.s are not accessible, as in most turbo-generator sets, then equation (4) may be used to obtain responses at rotor internal d.o.f. from measured bearing location responses in conjunction with known unbalances for the different unbalance configurations.

For this a minimum of three run-down responses are required (it is assumed here that the rotor-bearing system will always have some unknown residual unbalance); one run-down without trial mass (but with unknown residual unbalance) and two run-downs with trial masses (known additional unbalance).

3. REGULARIZATION

The condition of the matrices to be inverted in equation (17) should be taken into account, and the condition number (ratio of the maximum singular value to the minimum singular value) may be improved by pre-conditioning or by scaling parameters. Column scaling is necessary because of the different magnitudes of the elements of the $(\mathbf{K}_B - \omega_i^2 \mathbf{M}_B)$ and $\mathbf{C}_B$ matrices, and the scaling factors used are 1 and ω_i, respectively, where ω_i represents the rotor speed at which bearing parameters are estimated. Row scaling is not required here since the identification is performed at a particular speed, so the magnitude of the forces do not change much, as the chosen unbalances vary little in practice. It is observed that equation (17) is an ill-posed problem when the orbit of the rotor at bearings is circular or nearly circular (see Appendix A for a detailed explanation). Circular orbits of symmetrical rotors are expected for isotropic bearings. The test rig used for validation of the present algorithm has nearly isotropic bearings and has nearly circular orbits for a wide range of rotor speeds. For elliptical orbits, i.e., for anisotropic bearings, equation (17) is usually well-conditioned.

The Tikhonov and Arsenin [14] regularization technique was used to solve the ill-posed equations. The *discrete Tikhonov-regularization problem* equivalent to equation (17) is the least-squares problem

$$\beta_\lambda = min\{\|\mathbf{B}\boldsymbol{\beta} - \mathbf{q}\|^2 + \lambda^2 \|\mathbf{L}\boldsymbol{\beta}\|^2\}, \tag{19}$$

where $\|\cdot\|$ represents the matrix 2-norm, λ is the regularization parameter and L is the regularization matrix. Typical forms of the regularization matrix are the identity matrix or a well-conditioned discrete approximation to some derivative operator. The regularization parameter and matrix control the smoothness of the solution. The most convenient graphical tool for the selection of the regularization parameter, λ, for the analysis of ill-posed problems is the so-called *L-curve* which is a plot (for all valid regularization parameters) of the 2-norm $\|\mathbf{L}\boldsymbol{\beta}\|$ of the regularized solution versus the corresponding residual 2-norm $\|\mathbf{B}\boldsymbol{\beta} - \mathbf{q}\|$. This plot has a characteristic *L-shaped* appearance with a distinct corner separating the vertical and horizontal parts of the curve. In this way, the L-curve clearly displays the compromise between minimization of these two quantities, which is the heart of any regularization method. The regularization parameter corresponding to the corner of the L-curve corresponds to the optimum regularization parameter. The regularized solution is obtained by using the generalized SVD of the matrix pair (**B**, **L**).

For nearly isotropic bearings, where the orbits become nearly circular and equation (17) is an ill-posed problem, regularization may be performed by minimizing the square of the difference between the bearing parameters in the horizontal and vertical directions. A regularization parameter and matrix of the following form may be used:

$$\lambda\mathbf{L} = \begin{bmatrix} \lambda_k & 0 & 0 & -\lambda_k & 0 & 0 & 0 & 0 \\ 0 & \lambda_k & -\lambda_k & 0 & 0 & 0 & 0 & 0 \\ 0 & 0 & 0 & 0 & \lambda_c & 0 & 0 & -\lambda_c \\ 0 & 0 & 0 & 0 & 0 & \lambda_c & -\lambda_c & 0 \end{bmatrix}, \tag{20}$$

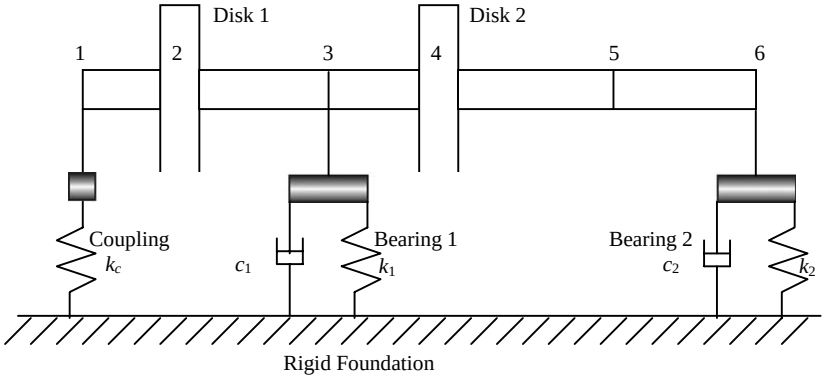

Figure 2. Schematic diagram of the test rig rotor-bearings-coupling model.

where λ_k and λ_c are the regularization parameters for the stiffness and damping parameters respectively. This regularization minimizes the difference in the direct and cross stiffness and damping terms. Section 5 illustrates regularization for nearly isotropic bearing in a more detail.

4. EXPERIMENTAL ROTOR-BEARING RIG

An experimental rotor-bearing rig at the University of Wales Swansea is used to validate the proposed algorithm for the identification of speed-dependent bearing parameters. Figure 2 shows a schematic diagram of the test rig. A simple flexible rotor was supported on two flexible bearings with a rigid foundation. The flexible bearings consist of effectively rigid rolling element bearings with the outer race attached to a relatively light bearing housing and that is, in turn, supported on flexible springs attached to a rigid foundation. Accelerometers were mounted at each bearing housing measuring the horizontal and vertical direction responses of the bearings (i.e., the responses at the connection d.o.f.s between the shaft and the rigid foundation). A variable speed motor drives the rotor through a flexible coupling. Two rigid discs were mounted on the rotor at distances of 79 and 459 mm, respectively, measured from the coupling, whilst bearings 1 and 2 were at distances of 234 and 733 mm. 1 and 2 refer to the drive-side and free-end of the rotor respectively. The rotor was a steel shaft 750 mm long and 12 mm nominal diameter. The steel discs had an internal diameter of 12 m m, an outside diameter of 74 mm and 15 mm thickness. There were 16 equally spaced threaded holes in each disc at a radius of 30 mm, to allow for the addition of balance weights. The identification method detailed above requires frequency-based measurements of the rotor response at the bearing housing, over a controlled run-up or run-down of the machine. The objective of the measurement system was therefore to return a first order response, as only the synchronous response was required. A detailed description of the test rig and associated measurement and conditioning hardware can be found in reference [15].

5. SIMULATED EXAMPLE

The test rig discussed above was used for a simulated example. A finite element model of the rotor was created using 5 two-noded Timoshenko beam elements with gyroscopic

effects included, each with two translational and two rotational degrees of freedom (see Figure 2). The coupling was modelled as a simple direct-stiffness spring support whilst each of the bearings was modelled using 12 linear coefficients of mass, stiffness and damping. The dimensions of the rotor at each station are given in Table 1. The dynamic stiffness in equation (1) was simulated in the frequency interval of 10–60 Hz to get first order responses (run-downs or run-ups) corresponding to different unbalance configurations (see Table 2) for the assumed coupling and bearings parameters as given in Table 3. The coupling and bearing parameters have realistic values, similar to the actual test rig [15], although the damping parameters were chosen to give a small positive damping.

TABLE 1

Details of the rotor model for the simulated and experimental examples

Station	Distance from coupling (mm)	Element length (mm)
1. (coupling)	0	—
2. (disk 1)	79	79
3. (bearing 1)	234	155
4. (disk 2)	459	225
5. (shaft intermediate point)	596	137
6. (bearing 2)	733	137

TABLE 2

Different unbalance configurations used for the simulated example

Configuration	Disc 1			Disc 2		
	Mass (kg)	Radius (mm)	Phase (deg)	Mass (kg)	Radius (mm)	Phase (deg)
I	0·001	30	0	0·003	30	60
II	0·003	30	0	0·001	30	60

TABLE 3

Details of coupling and bearing parameters assumed for the simulated example

Parameters		Coupling	Bearing 1	Bearing 2
Mass (kg)	m_{xx}	0·066	0·447	0·370
	m_{xy}	0·000	0.039	− 0·013
	m_{yy}	0·066	0·459	0·364
	m_{yx}	0·000	0·039	− 0·013
Stiffness (N/m)	k_{xx}	9000	16 788	17 070
	k_{xy}	0	1000	− 396
	k_{yy}	9000	18 592	16 920
	k_{yx}	0	1000	− 396
Damping (N s/m)	c_{xx}	0	6·00	3·00
	c_{xy}	0	0·00	0·00
	c_{yy}	0	6·00	3·00
	c_{yx}	0	0·00	0·00

The simulated responses corresponding to unbalance configurations I and II were substituted into equation (17) to estimate the speed-dependent bearing parameters. Initially, the ordinary least-squares method was used and the bearing parameters were accurately estimated. For simulation the assumed damping cross-coupled terms, as given in Table 3, were chosen to be zero, whilst the estimated damping cross-coupled terms were less than 10^{-8}. The estimated bearing parameters were used to estimate the response from equation (1) in conjunction with the unbalance configuration information. As expected the amplitude and phase responses for the simulated and estimated cases matched very closely.

In order to check the robustness of the present algorithm the bearing responses were contaminated with noise during estimation. When the least-squares method was used to solve equation (17), Figures 3 and 4 show the assumed and estimated bearing parameters with respect to rotor speed for bearing 2, when 1% random noise was added to the simulated bearing responses. Large errors in the estimated parameters were found in some of the speed ranges as compared to the chosen parameters. In order to ascertain the cause of these parameter errors, a plot of the variation in the bearing response amplitude ratio in the horizontal and vertical directions is shown in Figure 5 for both the bearings 1 and 2. It clearly shows that in most of the speed range the orbit is nearly circular (amplitude ratio is nearly equal to unity). Thus, in most of the speed range the estimation equations were ill-conditioned (see Appendix A) except near the resonances where the orbits were elliptical. To check the robustness of the present algorithm against noise for elliptical orbits, the simulation was repeated for changed bearing parameters (i.e., taking $k_{yy} = 2k_{xx}$ for both the bearings), when 1% random noise was added to the simulated bearing responses. Figures 6 and 7 show the corresponding assumed and estimated bearing parameters with non-regularized ordinary least squares for bearing 2. The reasonably good agreement

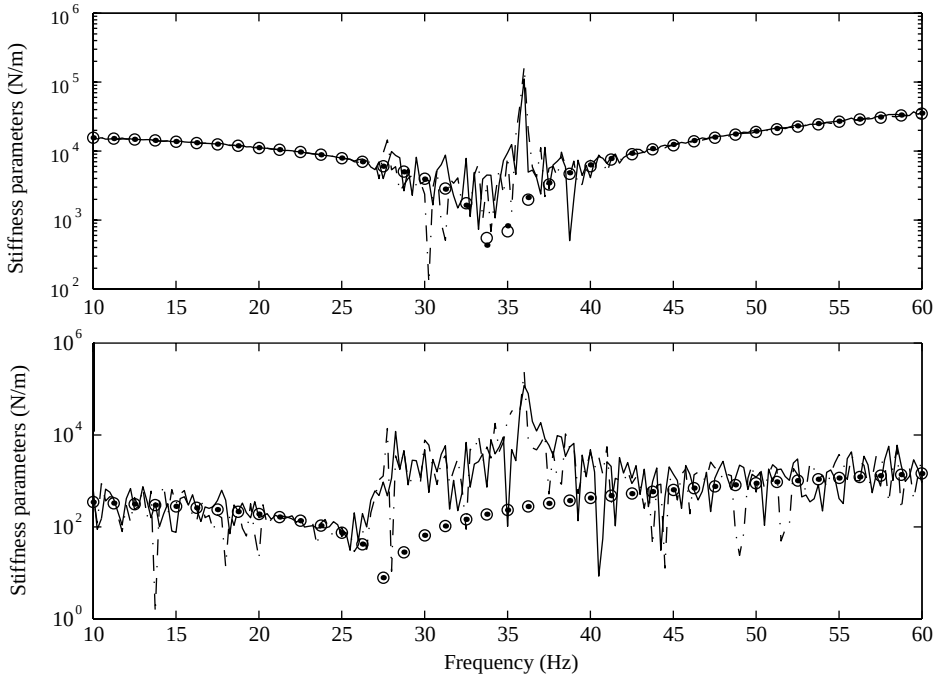

Figure 3. Comparison of the assumed and estimated (non-regularized) effective sepsfness parameters of bearing 2 with noise in the simulated bearing response.

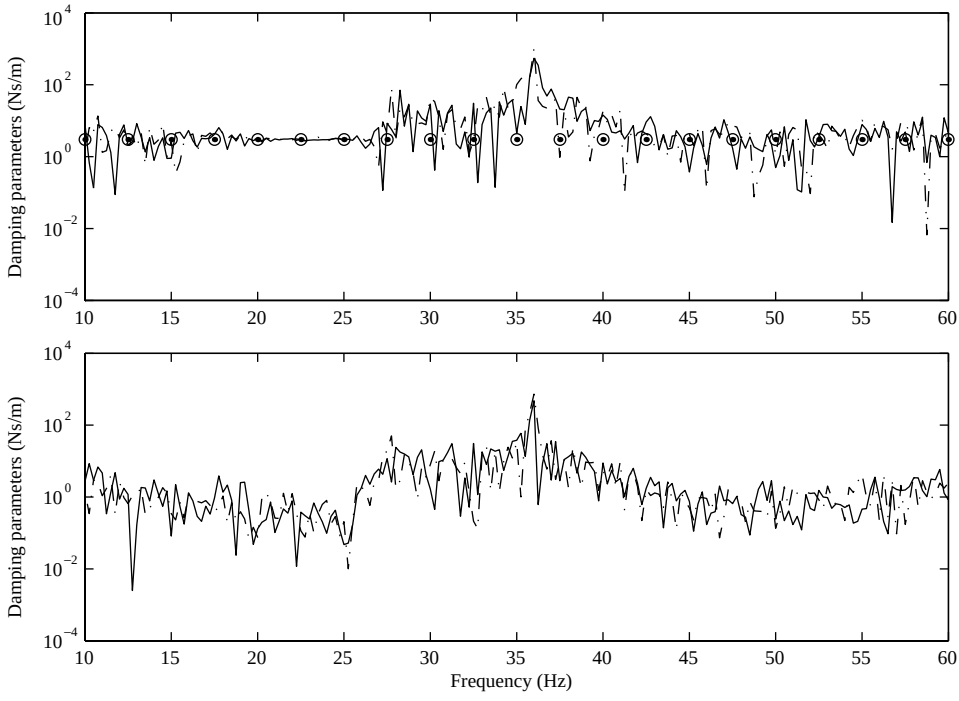

Figure 4. Comparison of the assumed and estimated (non-regularized) damping parameters of bearing 2 with noise in the simulated bearing response.

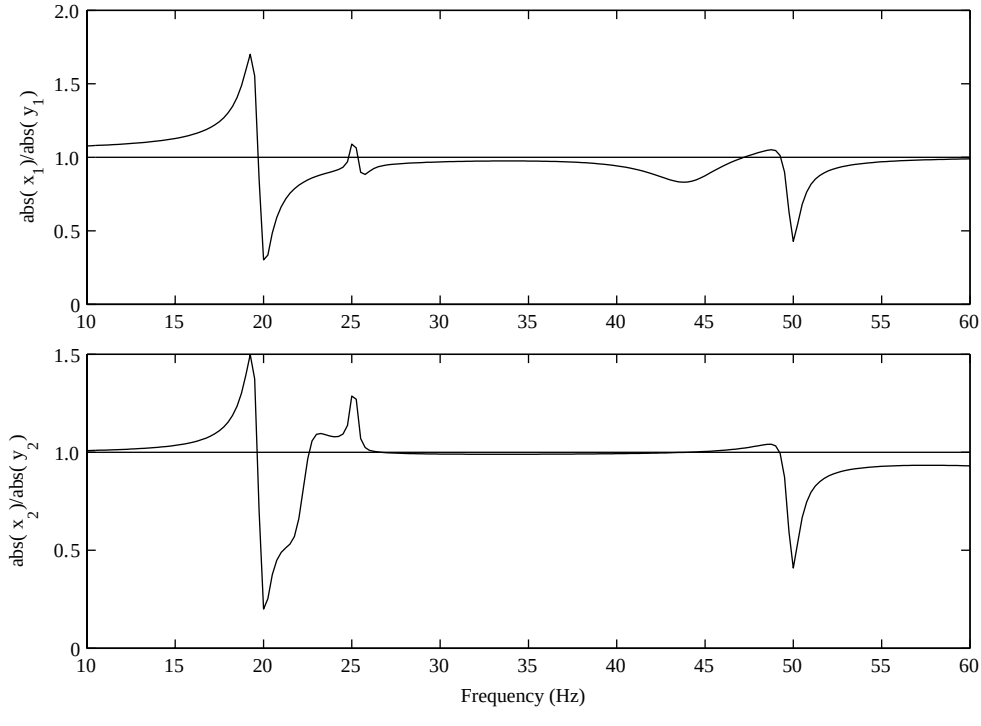

Figure 5. Simulated bearing response amplitude ratio in the horizontal and vertical directions, at bearing 1 and 2.

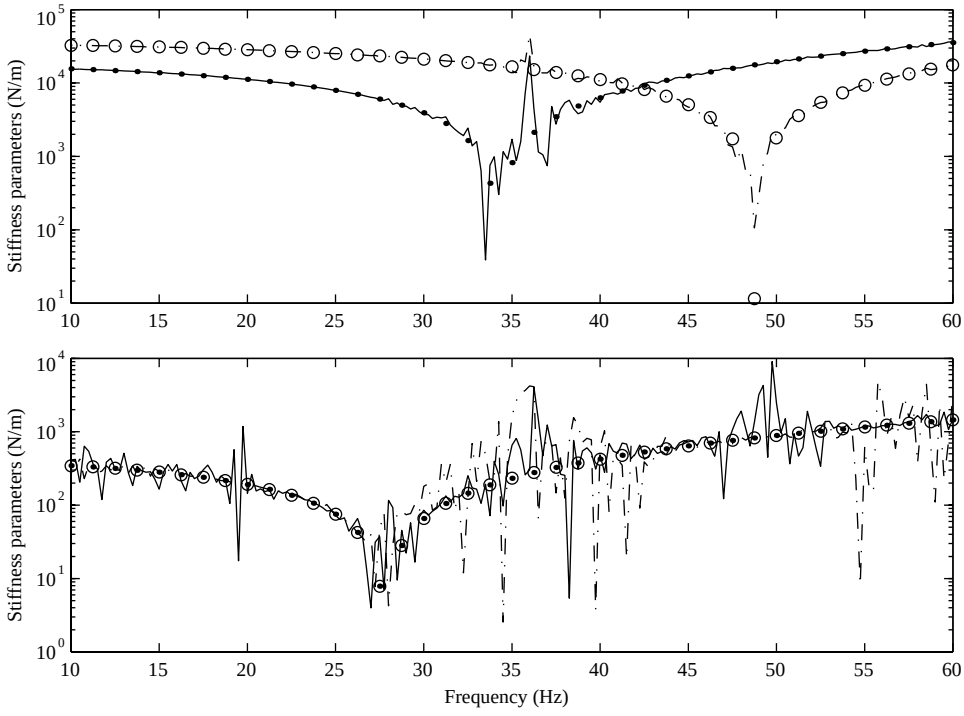

Figure 6. Comparison of the assumed and estimated (non-regularized) effective sepsfness parameters of bearing 2 with noise in the simulated bearing response for $k_{yy} = 2k_{xx}$.

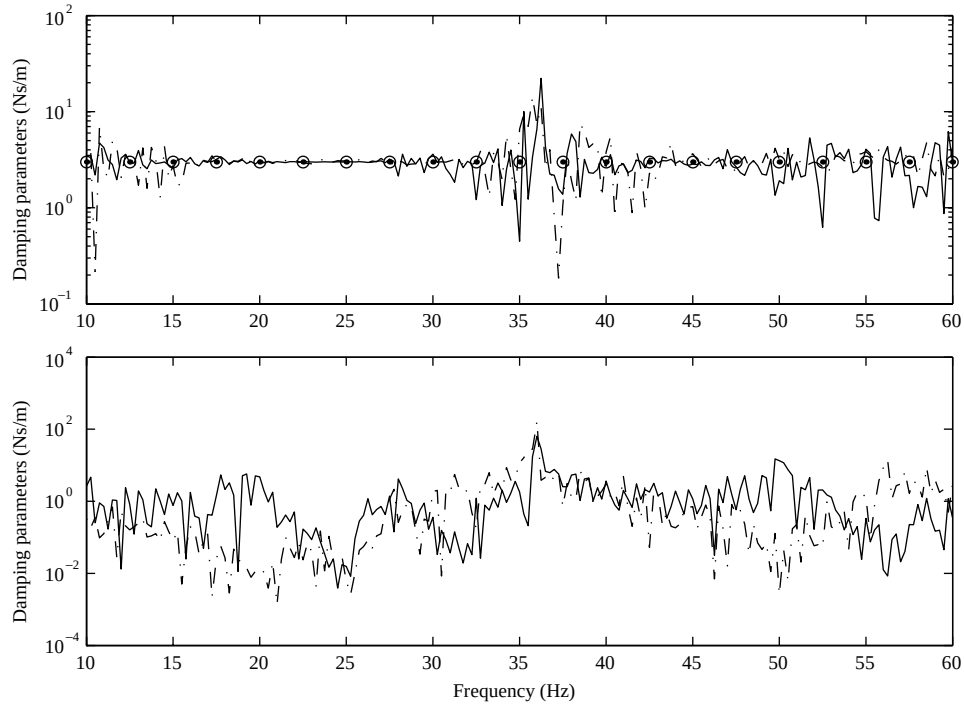

Figure 7. Comparison of the assumed and estimated (non-regularized) damping parameters of bearing 2 with noise in the simulated bearing response for $k_{yy} = 2k_{xx}$.

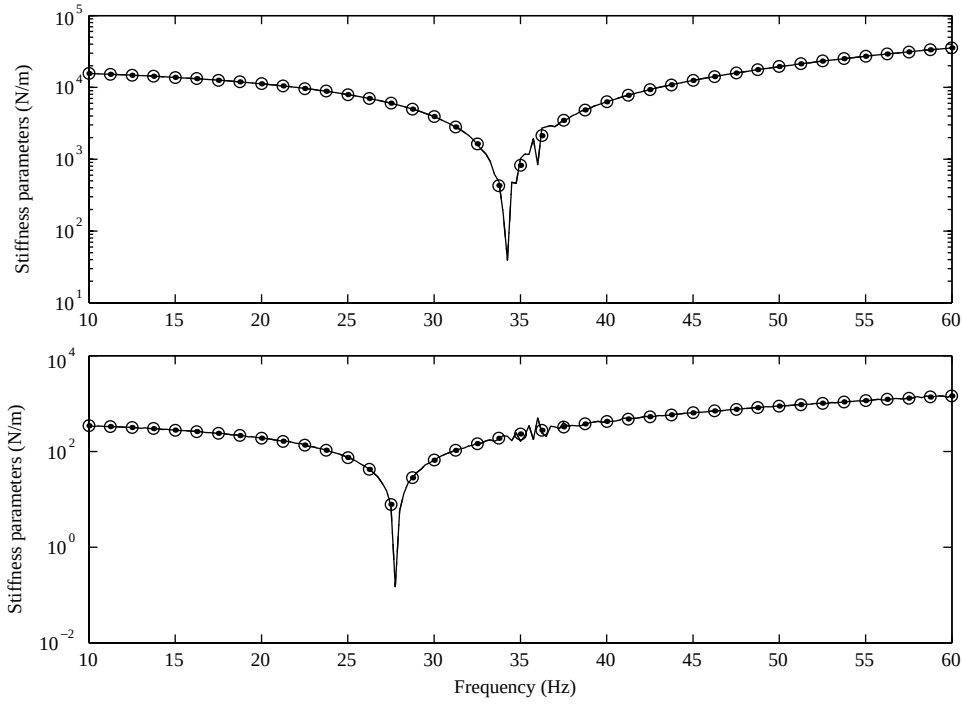

Figure 8. Comparison of the assumed and estimated (regularized as isotropic bearing) effective sepsfness parameters of bearing 2 with noise in the simulated bearing response.

suggests the robustness of present algorithm against noise for elliptical orbits. Since the present algorithm was found to be well-conditioned for the elliptical orbits, it was decided that regularization should only be used when required. In all of the examples, the measurement noise has caused the estimates of the damping cross terms to become non-zero. However, the cross terms are generally smaller in magnitude than the direct terms, and in any case the damping in the system is very small.

Since the present example has nearly isotropic bearings and in most of the range the orbits are nearly circular, regularization was used for isotropic bearings as discussed in section 3. To demonstrate the method perfectly isotropic bearings were considered. Figures 8 and 9 show the corresponding assumed and estimated bearing parameter variation for bearing 2, for perfectly isotropic bearings, with respect to the rotor speed. For regularization, the regularization parameters (λ_k and λ_c) were set to 10^{-1}. Excellent agreement has been found between the simulated and estimated bearing parameters, even in the presence of noise in the simulated bearing responses, and this demonstrates the robustness of the present method against noise. When more unbalance configurations were used for the bearing parameter estimation, the accuracy of the estimated bearing parameters improves, especially in the presence of noise in simulated response. For experimental data where the presence of noise is unavoidable, estimating bearing parameters by using more than two run-down responses would lead to improved estimates.

The method for the case when measurements are taken by rotating the rotor both in the clockwise and anticlockwise directions is discussed in Appendix A. To demonstrate the approach responses were generated and contaminated with noise. For unbalance configuration II the direction of rotation of the shaft was clockwise and for unbalance

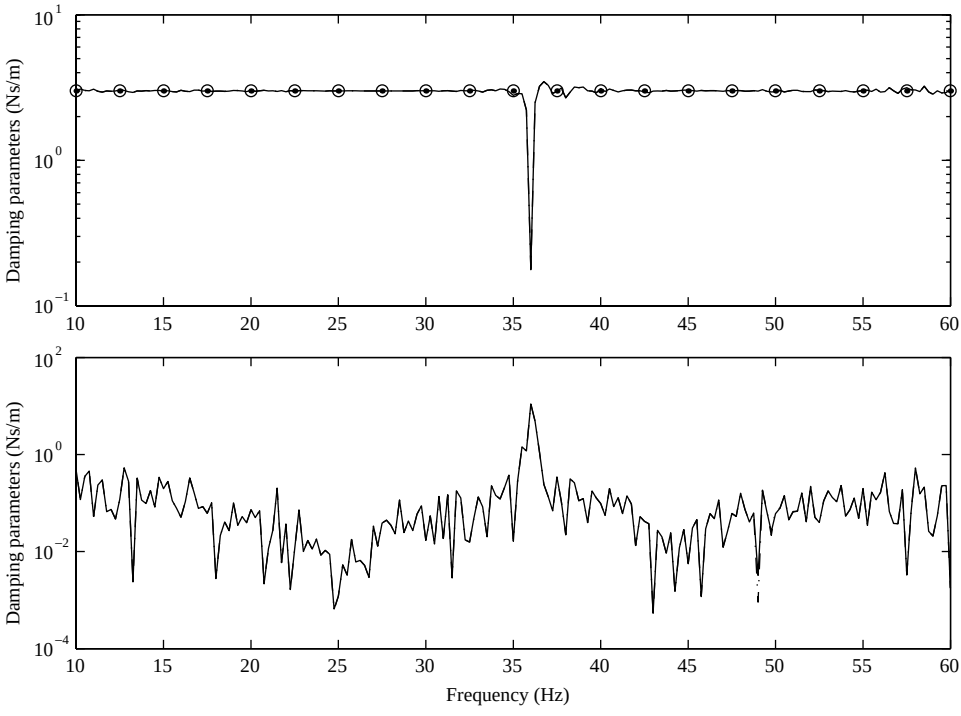

Figure 9. Comparison of the assumed and estimated (regularized as isotropic bearing) damping parameters of bearing 2 with noise in the simulated bearing response.

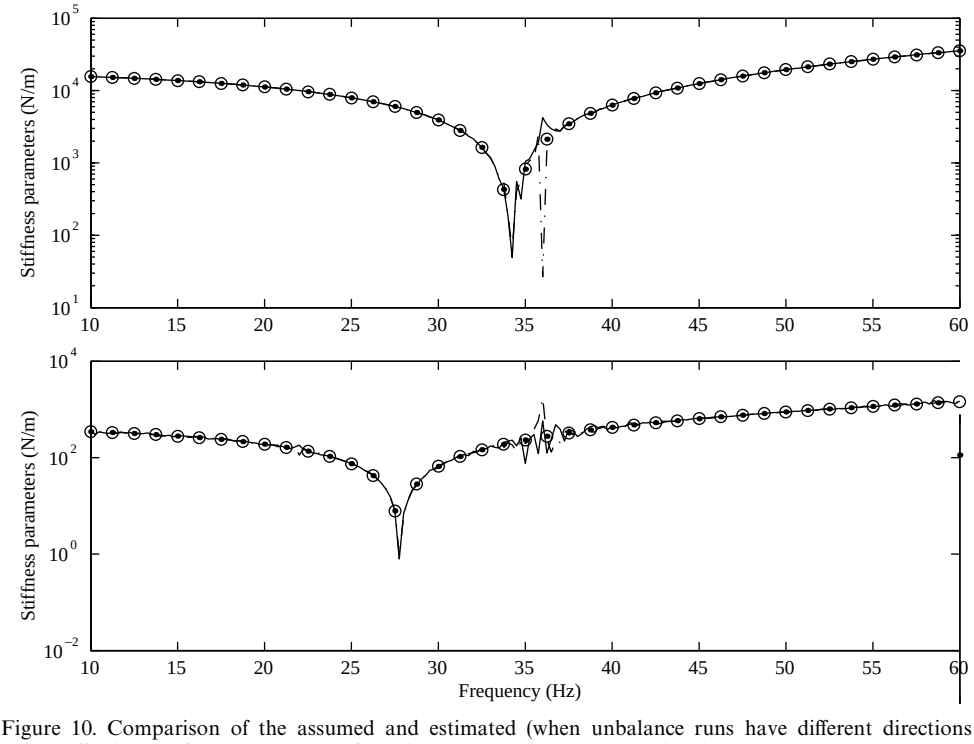

Figure 10. Comparison of the assumed and estimated (when unbalance runs have different directions of rotation) effective sepsfness parameters of bearing 2 with noise in the simulated bearing response.

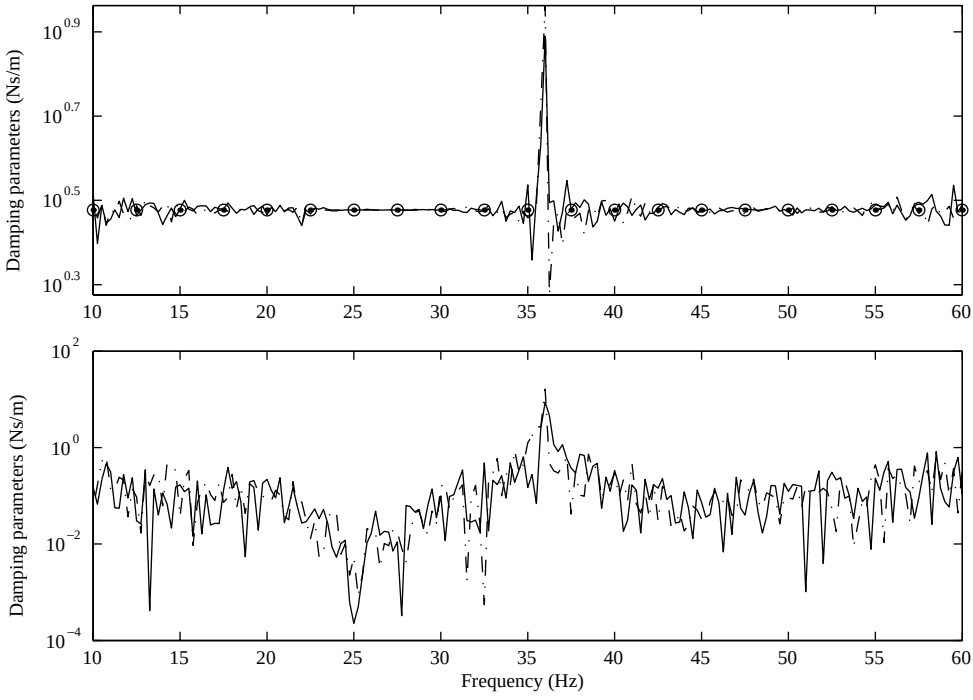

Figure 11. Comparison of the assumed and estimated (when unbalance runs have different directions of rotation) damping parameters of bearing 2 with noise in the simulated bearing response.

configuration I it was anticlockwise. The bearing parameters were estimated using the non-regularized ordinary least-squares method. A substantial reduction in the condition number of the regression matrix was found, and the maximum reduction was of the order of 10^3. Figures 10 and 11 show the corresponding assumed and estimated bearing parameter variation of bearing 2, for perfectly isotropic bearings, with respect to rotor speed. The estimated parameters show excellent agreement with the simulated bearing parameters and, even in the presence of noise in the simulated bearing responses, and this demonstrates the robustness of the method against noise.

6. EXPERIMENTAL RESULTS

The identification method was tested on experimental data from a test rig at the University of Wales Swansea. The finite element model of the rotor was identical to that discussed in the previous section. Since the main objective of the present work is to identify bearing parameters, the rotor and coupling parameters were taken as those given in Tables 1 and 3. The machine was run-down for different unbalance configurations from 44 to 15 Hz. The first order responses (displacements) in the horizontal and vertical directions at the bearing housings were extracted. The present algorithm requires responses measured at the same speeds for different runs and these were obtained from the experimental data for different runs by linear interpolation. However, modern order tracking analyser systems are able to measure data at any desired speed step and so eliminate this approximation. A speed step of 0·25 Hz was used for the interpolation of experimental bearing responses. Three runs were

TABLE 4

Different unbalance configurations used in the experimental example

Configuration	Disc 1			Disc 2		
	Mass (kg)	Radius (mm)	Phase (deg)	Mass (kg)	Radius (mm)	Phase (deg)
I (residual unbalance)	—	—	—	—	—	—
II	0·002	30	78·75	0·002	30	348·75
III	0·00123	30	101·25	0·0018	30	11·25

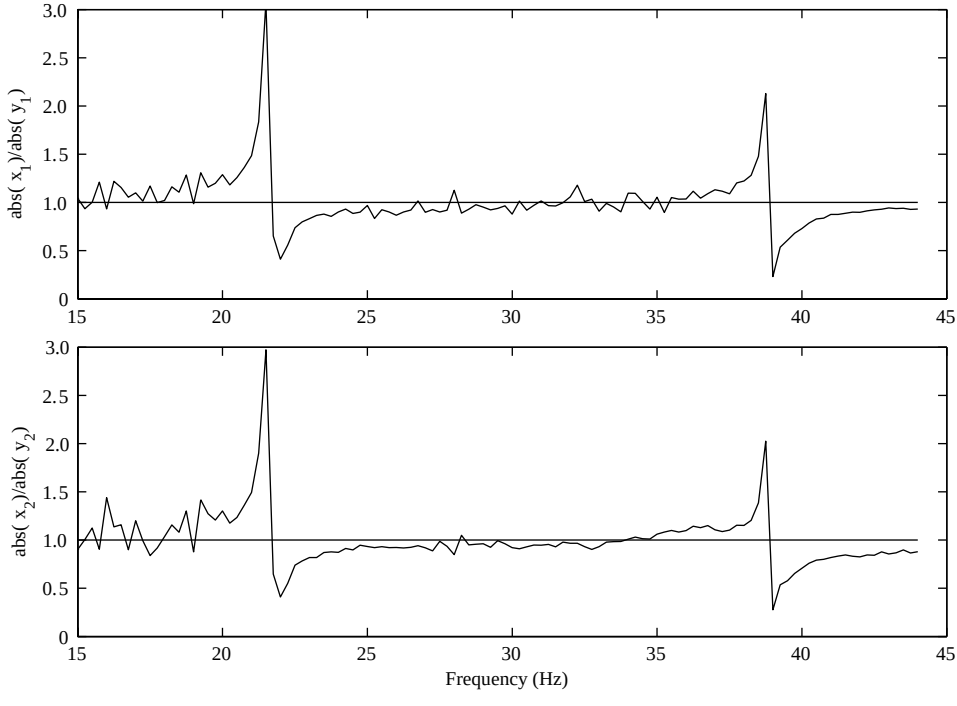

Figure 12. Experimental bearing response amplitude ratio in the horizontal and vertical directions, at bearing 1 and 2.

performed, the first with residual unbalance and the second and third cases with the addition of different unbalance configurations (see Table 4). Since the residual unbalance was unknown, the response for run 1 was subtracted for that of run 2 and run 3. Assuming the system is linear then the resulting responses will correspond to those arising from the added unbalances. The resulting bearing responses were used in equation (4) to obtain responses at the rotor internal d.o.f.s. The resulting responses and corresponding additional unbalance information were substituted into equation (17) to calculate the speed-dependent bearing parameters.

A plot of the variation of the bearing response amplitude ratio in the horizontal and vertical directions is shown in Figure 12, for both bearings 1 and 2. Figure 12 clearly shows

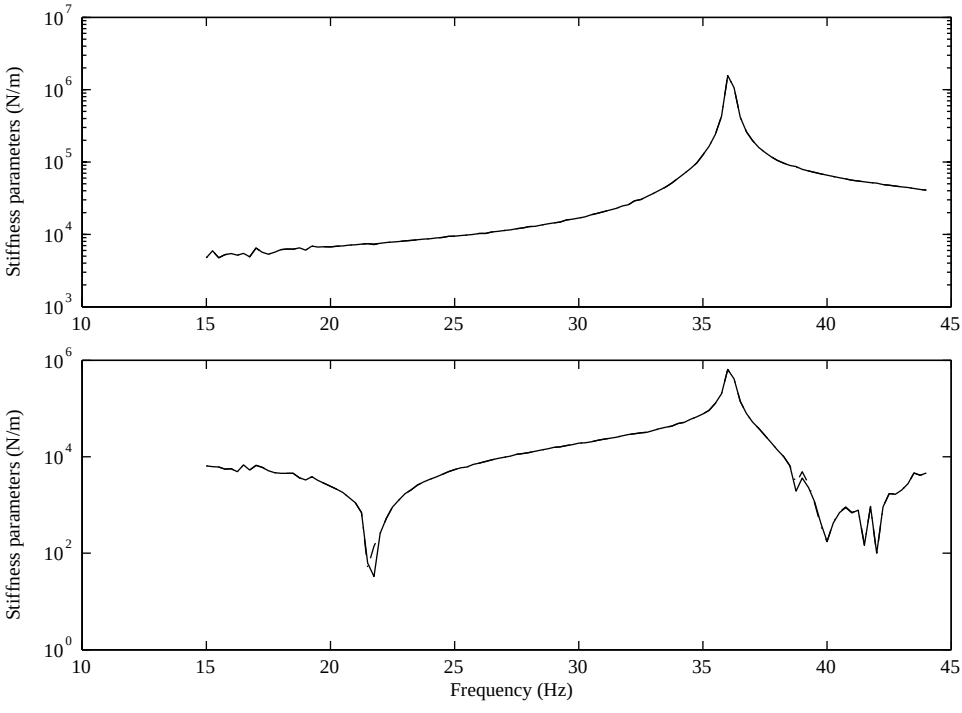

Figure 13. Estimated effective sepsfness parameters from the experimental responses for bearing 2 (regularized as isotropic bearing).

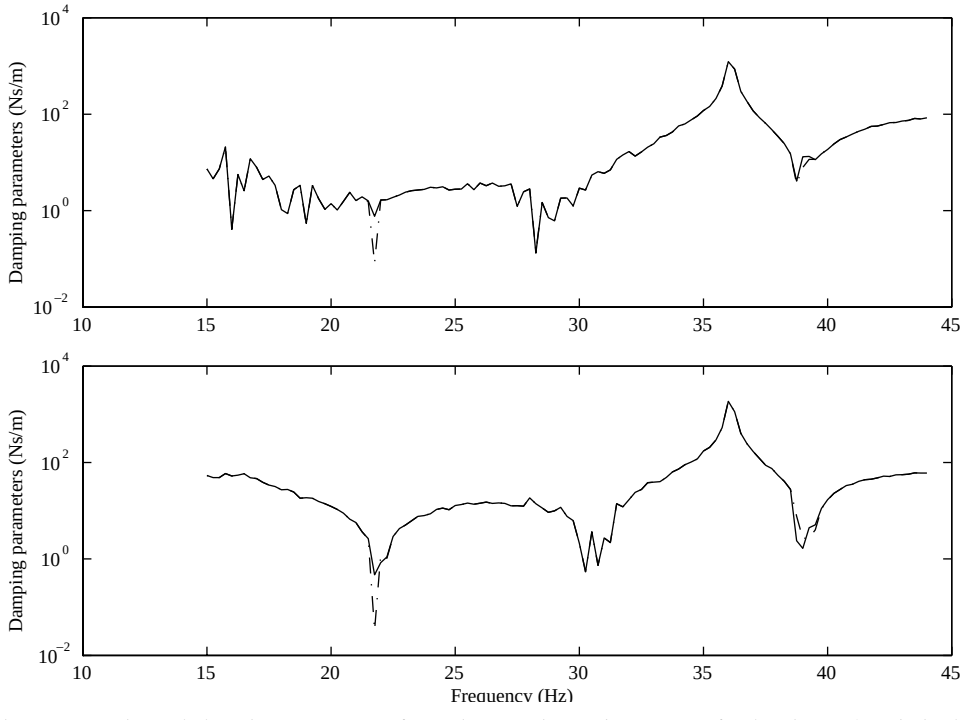

Figure 14. Estimated damping parameters from the experimental responses for bearing 2 (regularized as isotropic bearing).

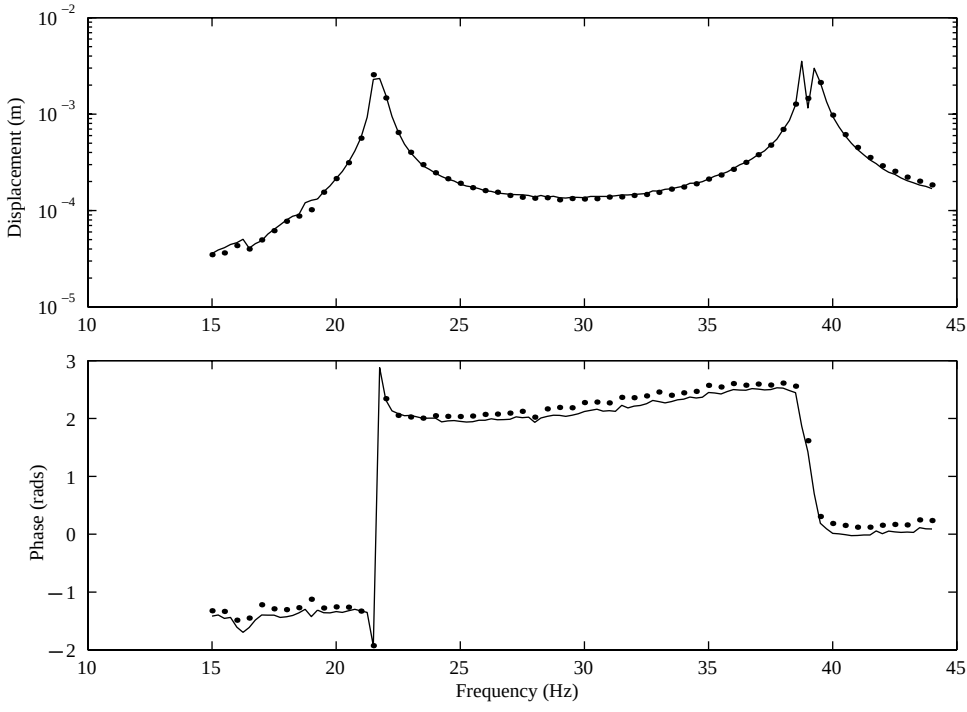

Figure 15. Experimental and estimated amplitude and phase responses (horizontal direction), at bearing 2, for unbalance configuration II.

that in most of the speed range the orbit is nearly circular (the amplitude ratio is nearly equal to unity with rapid fluctuations) except near the resonances. For regularization, a second order derivative operator (as discussed in section 3) along with a regularization parameter value of 10^{-1} was used, and was selected based on a trade-off between smoothing of the estimated parameters and response reproduction capabilities. Figures 13 and 14 show the variation of the estimated bearing effective stiffness and damping parameters (regularized as an isotropic bearing) with respect to the rotor speed. The estimated bearing parameters were used to obtain the estimated response by using equation (1) in conjunction with the unbalance information. Figures 15 and 16 show the comparison of the experimental and estimated bearing amplitude and phase variation for bearing 2 with respect to the rotor speed for unbalance configuration II, in the horizontal and vertical directions. Excellent reproduction of the responses shows the robustness of the present algorithm for the experimental data. Throughout the estimation bearing 2 was considered since it was expected to be a more representative check of the present algorithm since it was further from the coupling.

Using the present algorithm bearing parameters were estimated. The response reproduction capability of the estimated model was found to be excellent with responses from only three run-downs, i.e., one with residual unbalance and another two with known unbalances. For large rotating machines where measurement noise is expected to be higher, it is suggested that more unbalance configurations could be incorporated into the estimation.

7. CONCLUSIONS

An identification algorithm for the estimation of bearing speed-dependent dynamic parameters of flexible rotor-bearing systems has been presented. The estimation uses

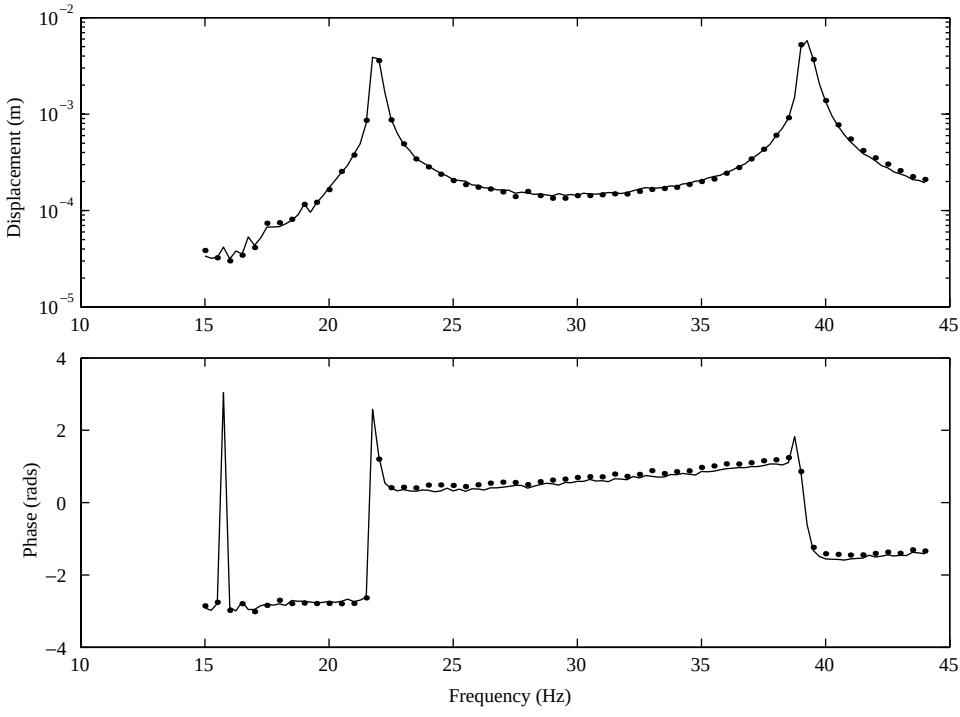

Figure 16. Experimental and estimated amplitude and phase responses (vertical direction), at bearing 2, for unbalance configuration II.

measured vibration data at the bearing housing from a minimum of two run-downs or run-ups of the machine in conjunction with the knowledge of the corresponding unbalance. The method is fully tested on simulated and experimental data from a two-bearing machine. For anisotropic bearings (elliptical orbits) the method is found to be robust to measurement noise. Bearing parameter estimation for nearly isotropic bearings (i.e., nearly circular orbits), which is an ill-posed problem, is successfully obtained using a combination of regularization and generalized SVD techniques. It is suggested that the ill-posed problem due to a circular orbit may be made well-conditioned by taking measurements with the rotor rotating in both the clockwise and anticlockwise directions. Bearing parameters are estimated and the response reproduction capabilities are very encouraging and it is envisaged that the main thrust of the future work should be the application of the identification to large machines with fluid-film bearings (i.e., turbo-generators). In the case of fluid-film bearings it would not be possible to run the system in the opposite direction of rotation since this would cause the bearing parameters to change. However, the fluid-film bearings dynamic characteristics are anisotropic in nature and the present algorithm works well for the anisotropic bearings. It would also be interesting to investigate the effects of foundation flexibility and shaft misalignment on the parameters estimates, and eventually the overall response.

ACKNOWLEDGMENTS

The authors acknowledge Dr S. Edwards, Department of Mechanical Engineering, University of Wales Swansea, U.K. for the experimental data used in the present work.

REFERENCES

1. M. G. SMART 1998 *Ph.D. Thesis, University of Wales Swansea*, U.K. Identification of flexible turbogenerator foundations.
2. J. R. MITCHELL, R. HOLMES and H. VAN BALLEGOOYEN 1966 *Proceedings of the Institution of Mechanical Engineers* **180** Part 3k. Experimental determination of a bearing oil film stiffness.
3. P. G. MORTON 1971 *Transactions of American Society of Mechanical Engineers, Journal of Lubrication Technology* **93**, 143–150. Measurement of the dynamic characteristics of large sleeve bearings.
4. D. CHILDS and K. HALE 1993 *STLE/ASME Vibration Conference: New Orleans, LA*. A test apparatus and facility to identify the rotordynamic coefficients of high speed hydrostatic bearings.
5. R. NORDMANN and K. SCHOLLHORN 1980 *Institution of Mechanical Engineers Conference Vibrations in Rotating Machinery: Cambridge*. Identification of stiffness and damping coefficients of journal bearings by means of the impact method.
6. J. KRAUS, J. J. BLECH and S. G. BRAUN 1987 *Transactions of American Society of Mechanical Engineers, Journal of Vibration, Acoustics, Stress, and Reliability in Design* **109**, 235–240. In situ determination of rolling bearing stiffness and damping by modal analysis.
7. M. N. SAHINKAYA and C. R. BURROWS 1984 *Proceedings of the Institution of Mechanical Engineers* **198c**, 131. Estimation of linearised oil film parameters from the out-of-balance response.
8. A. K. TIEU and Z. L. QIU 1994 *WEAR* **177**, 63–69. Identification of sixteen dynamic coefficients from experimental unbalance responses.
9. J. H. CHEN and A. C. LEE 1997 *Transactions of American Society of Mechanical Engineers, Journal of Vibration and Acoustics* **119**, 60–69. Identification of linearised dynamic coefficients of rolling element bearings.
10. A. MUSZYNSKA and D. E. BENTLY 1990 *Journal of Sound and Vibration* **143**, 103–124. Frequency-swept rotating input perturbation techniques and identification of the fluid force models in rotor/bearing/seal systems and fluid handling machines.
11. R. TIWARI and N. S. VYAS 1995 *Journal of Sound and Vibration* **187**, 229–239. Estimation of nonlinear stiffness parameters of rolling element bearings from random response of rotor bearing systems.
12. M. J. GOODWIN 1991 *Transactions of the American Society of Mechanical Engineers, Journal of Engineering for Industry* **113**, 335–342. Experimental techniques for bearing impedance measurement.
13. E. E. SWANSON and R. G. KIRK 1997 *Transactions of the American Society of Mechanical Engineers, Journal of Tribology* **119**, 704–710. Survey of experimental data for fixed geometry hydrodynamic journal bearings.
14. A. N. TIKHONOV and V. Y. ARSENIN 1977 *Solutions of Ill-Posed Problems*, Washington, DC: Winston & Sons.
15. S. EDWARDS, A. W. LEES and M. I. FRISWELL 2000 *Journal of Sound and Vibration* **232**, 963–992. Experimental identification of excitation and support parameters of a flexible rotor-bearings–foundation system from a single run-down.

APPENDIX A: CONDITIONING OF BEARING ESTIMATION

Consider equation (6) for a single bearing and use a complex stiffness at a single frequency. Let

$$H_B = K_B(\omega) - (\mathrm{j}\omega)^2 M_B + \mathrm{j}\omega C_B = \begin{bmatrix} k_{xx} & k_{xy} \\ k_{yx} & k_{yy} \end{bmatrix}. \tag{A1}$$

Then, the dynamic equation may be written as

$$\begin{bmatrix} k_{xx} & k_{xy} \\ k_{yx} & k_{yy} \end{bmatrix} \begin{Bmatrix} x \\ y \end{Bmatrix} = \begin{Bmatrix} P_x \\ P_y \end{Bmatrix}. \tag{A2}$$

Using two unbalance runs with corresponding responses x_1, y_1, x_2 and y_2 and right-hand sides P_{x1}, P_{y1}, P_{x2} and P_{y2}, equation (A2) may be written as

$$\begin{bmatrix} k_{xx} & k_{xy} \\ k_{yx} & k_{yy} \end{bmatrix} \begin{bmatrix} x_1 & x_2 \\ y_1 & y_2 \end{bmatrix} = \begin{bmatrix} P_{x_1} & P_{x_2} \\ P_{y_1} & P_{y_2} \end{bmatrix}. \tag{A3}$$

The solution is obtained as

$$\begin{bmatrix} k_{xx}\, k_{xy} \\ k_{yx}\, k_{yy} \end{bmatrix} = \frac{1}{(x_1 y_2 - x_2 y_1)} \begin{bmatrix} P_{x_1}\, P_{x_2} \\ P_{y_1}\, P_{y_2} \end{bmatrix} \begin{bmatrix} y_2 & -x_2 \\ -y_1 & x_1 \end{bmatrix}. \tag{A4}$$

For circular orbits $y_1 = \mathrm{j}x_1$ and $y_2 = \mathrm{j}x_2$ (or $-$ ve, depends on the definition of axes, and the direction of rotation). Then the denominator of equation (A4) becomes

$$x_1 y_2 - x_2 y_1 = x_1(\mathrm{j}x_2) - x_2(\mathrm{j}x_1) = 0 \tag{A5}$$

and hence, equation (A4) is ill-conditioned for circular orbits.

Having a third unbalance run does not help. For three unbalances equation (A2) may be written as

$$\begin{bmatrix} k_{xx} & k_{xy} \\ k_{yx} & k_{yy} \end{bmatrix} \begin{bmatrix} x_1 & x_2 & x_3 \\ y_1 & y_2 & y_3 \end{bmatrix} = \begin{bmatrix} P_{x_1} & P_{x_2} & P_{x_3} \\ P_{y_1} & P_{y_2} & P_{y_3} \end{bmatrix}. \tag{A6}$$

The least-squares solution involves the following inversion:

$$\left[\begin{bmatrix} x_1 & x_2 & x_3 \\ y_1 & y_2 & y_3 \end{bmatrix} \begin{bmatrix} x_1 & y_1 \\ x_2 & y_2 \\ x_3 & y_3 \end{bmatrix} \right]^{-1} = \begin{bmatrix} x_1^2 + x_2^2 + x_3^2 & x_1 y_1 + x_2 y_2 + x_3 y_3 \\ x_1 y_1 + x_2 y_2 + x_3 y_3 & y_1^2 + y_2^2 + y_3^2 \end{bmatrix}^{-1}$$

$$= \frac{1}{(x_1^2 + x_2^2 + x_3^2)(y_1^2 + y_2^2 + y_3^2) - (x_1 y_1 + x_2 y_2 + x_3 y_3)^2}$$

$$\times \begin{bmatrix} y_1^2 + y_2^2 + y_3^2 & -(x_1 y_1 + x_2 y_2 + x_3 y_3) \\ -(x_1 y_1 + x_2 y_2 + x_3 y_3) & x_1^2 + x_2^2 + x_3^2 \end{bmatrix} \tag{A7}$$

If $y_i = \mathrm{j}x_i$, then the denominator of equation (A7) becomes

$$(x_1^2 + x_2^2 + x_3^2)(y_1^2 + y_2^2 + y_3^2) - (x_1 y_1 + x_2 y_2 + x_3 y_3)^2$$
$$= (x_1^2 + x_2^2 + x_3^2)\,\mathrm{j}^2(x_1^2 + x_2^2 + x_3^2) - [\,\mathrm{j}(x_1^2 + x_2^2 + x_3^2)]^2 = 0 \tag{A8}$$

and the circular orbits are still ill-conditioned.

There is another possibility when ill-conditioning may occur, namely when $y_1 = \alpha x_1$ and $y_2 = \alpha x_2$ for any value of α, where α is a constant. Then the denominator of equation (A4) becomes zero, leading to ill-conditioning. This means that a change in orbit from one unbalance to the next is required.

The ill-conditioning due to a circular orbit may be avoided by taking measurements in both the clockwise and anticlockwise directions of rotation of the rotor. For this case $y_1 = \mathrm{j}x_1$ and $y_2 = -\mathrm{j}x_2$. Then the denominator of equation (A4) becomes

$$x_1 y_2 - x_2 y_1 = x_1(-\mathrm{j}x_2) - x_2(\mathrm{j}x_1) \neq 0 \tag{A9}$$

and hence, equation (A4) becomes well-conditioned.

APPENDIX B: NOMENCLATURE

B	regression matrix
D	dynamic stiffness, $(k - m\omega^2 + \mathrm{j}\omega c)$
f_u	unbalance force
j	$\sqrt{-1}$
K, **C**, **M**	stiffness, damping and mass matrices

$\mathbf{L}$	regularization matrix
m	number of unbalance configuration run-downs
n_b	total number of bearings in the rotor-bearing system
x, y	bearing responses in the horizontal and vertical directions respectively
$\mathbf{z}$	d.o.f.s of the rotor, containing linear and angular displacements
$\mathbf{z}_{R,b}$	d.o.f.s of the rotor at the bearing locations
$\mathbf{z}_{R,i}$	d.o.f.s of the rotor other than at the bearing locations
λ	regularization parameter
ω	rotor running speed

Subscripts

b	rotor connection d.o.f.s
B	bearing
i	rotor internal d.o.f.s
R	rotor

Superscripts

i	imaginary part
r	real part